Supporting Information

for

A multifunctional nanoplatform combining self-supplied H_2O_2 production with CO delivery for multimodal anti-tumor therapy

Meng-Jie Chen,[a] Cheng-Bin Wang,[a] Hai-Lin Zhang,[a] Shi-Ping Yang,[b] Jin-Gang Liu [a,*]

[a]*Key Laboratory for Advanced Materials, School of Chemistry & Molecular Engineering,*

East China University of Science and Technology, Shanghai 200237, P. R. China

E-mail: liujingang@ecust.edu.cn

[b]*Key Lab of Resource Chemistry of MOE & Shanghai Key Lab of Rare Earth Functional Materials, Shanghai Normal University,*

Shanghai 200234, P. R. China.

Materials and Methods

Materials: All reagents were purchased commercially and used without further purification. [(tpy^{COOH})$Mn(CO)_2(Br)$] (MnCO) [S1] and the CO probe (FL-CO-1) [S2] were prepared according to the literatures.

Characterization Techniques: All test instruments are referred to our previous reports. [S1, S2]

Synthesis of CaO_2 NPs

The CaO_2 nanoparticles were synthesized via wet chemistry according to the previously reported methods.[S3] Briefly, $CaCl_2 \cdot 2H_2O$ (2.0 M, 1.0 mL) was added to 60 mL of absolute methanol under vigorous stirring at room temperature for 10 min to disperse in solvents thoroughly. Subsequently, 400 μL of $NH_3 \cdot H_2O$ (25% ~ 28%) was introduced into the mixture to provide an alkaline environment. Finally, 300 μL of 30% H_2O_2 was dropwise added and stirred for 30 min. They milky solution was collected by centrifugation at 10000 rpm for 10 min, washed, and centrifuged three times by methanol. At last, the product was dispersed in methanol at 4 ℃.

Synthesis of CaO_2@PDA and CaO_2@PDA-Cu

Firstly, the CaO_2 NPs (10 mg) were dispersed in the Tris-HCl buffer solution (pH = 8.5, 30 mL), to which dopamine (dispersed in water, 10 mg, 5 mg/mL) was added dropwise. Following a 3-hour interval, the initially milky white suspension underwent a gradual transformation into a dark black hue. The product CaO_2@PDA was collected after washing and centrifugation three times. Similarly, the CaO_2@PDA-Cu was prepared in the same way, and $CuCl_2$ (10 mg, 20 mg/mL) solution was swiftly added to the buffer solution during dopamine polymerization.

Synthesis of CaO_2@PDA-Cu@tpy^{COOH}MnCO

[(tpy^{COOH})$Mn(CO)_2(Br)$] (30 mg) was firstly dispersed in DMF and then activated by reaction with NHS and EDC for 1h at RT. The prepared CaO_2@PDA-Cu solution was added to the above solution and stirred for 24 h under dark. Following that, the resulting samples were washed and centrifuged several times with DMF and H_2O, and finally freeze-dried for subsequent use.

In vitro detection release of CO

The detection of CO followed the previous protocol.[S1, S2]

Measurement of photothermal performance

Firstly, the temperature variation of different solutions (H_2O, CaO_2, CaO_2@PDA, CaO_2@PDA-Cu, CaO_2@PDA-Cu@MnCO) under 808 nm laser irradiation was determined. Secondly, the temperature variation of the CaO_2@PDA-Cu@MnCO solution under different power densities (0.5, 1.0, 1.5 W/cm^2) conditions was measured. At the same time, the heating trend of the solution of CaO_2@PDA-Cu@MnCO in different concentrations (0~400 μg/mL) under 808 nm laser irradiation was also studied. Finally, the photothermal stability and photothermal conversion efficiency of CaO_2@PDA-Cu@MnCO were also explored.

Colorimetric identification of peroxy groups

The solution containing CaO_2, CaO_2@PDA, or H_2O_2 was added to the $KMnO_4$ (50 μg/mL) solution containing H_2SO_4 (0.1 M). Subsequently, its UV-vis absorption spectrum was examined in the wavelength range from 400 nm to 650 nm.

H_2O_2 Released from CaO_2

Ti $(SO_4)_2$ was used as an indicator of H_2O_2, which produced yellow precipitation of the peroxide-titanium complex. The precipitation could be dissolved by H_2SO_4 and determined at 410 nm within a certain range. Its absorbance was linear with the concentration of H_2O_2. After that, one milliliter of H_2O_2 solution with different concentrations (60, 100, 200, 400, 800, 1000, and 2000 μM) was added to the $Ti(SO_4)_2$ solution (4.8%). The UV-Vis absorption spectra of different concentrations of solution at 410 nm were determined, and the standard curves of $Ti(SO_4)_2$-H_2O_2 were obtained. The content of H_2O_2 produced by CaO_2 under acidic conditions was determined by $Ti(SO_4)_2$ colorimetry. One milligram of CaO_2 NPs was dispersed in 1 mL of solution with different pH values (7.4, 6.5, and 5.5). Subsequently, the supernatant was collected by centrifugation and mixed with $Ti(SO_4)_2$ solution. After that, the absorbance of different mixtures at 410 nm were examined, and the concentrations of H_2O_2 were determined using the standard curve of H_2O_2.

Detection of Hydroxyl radicals (•OH)

Electron Paramagnetic Resonance (EPR) was applied to validate the production of ·OH using 5, 5-dimethyl-1-pyrroline N-oxide (DMPO) as a spin trapping agent in Bruker A300. And ·OH production was also evaluated using the classical colorimetric method of degradation of methylene blue (MB), of which UV-vis absorption spectrum was recorded. Initially, different concentrations of CaO_2@PDA-Cu (0, 5, 10, 25, 50, 100 μg/mL) were added to a buffer solution (pH = 6.5) containing MB (10 μg/mL). After that, the solution was stirred at 37 ℃ for 4 h. Finally, its UV-vis absorption spectrum was examined from 400 nm to 800 nm.

•OH detection by photothermal enhancement

OPD could be easily oxidized by various oxidants to produce the yellow fluorescent substance OPDox, thereby facilitating the detection of ·OH formation using the traditional colorimetric method. Briefly, 1.0 mg of CaO_2@PDA-Cu NPs were dispersed in 1.0 mL pH 6.5 buffer solution and stirred for 4 h. Subsequently, the supernatant was collected by centrifugation and mixed with 1.0 mL of OPD solution. After that, the absorbance of different mixtures from 300 nm to 800 nm were recorded.

GSH depletion measurements

DTNB was used to measure the consumption of GSH, and different nanoparticles (CaO_2@PDA and CaO_2@PDA-Cu, 100 μg/mL) and GSH (2.0 mM) were stirred in PBS (pH 6.5) at 37 ℃ for 8 h. Subsequently, the indicator DTNB was introduced. Following a complex interaction between GSH and DTNB for a duration of 15 min, the absorbance shift at 410 nm was measured, allowing for the quantification of GSH consumption.

Intracellular free radical assessment

The DCFH-DA probe was used to detect intracellular production of free radicals. Briefly, 4T1 cells were cultured in 12-well plates for 24 h and treated with samples (PBS, CaO_2@PDA+Laser, CaO_2@PDA-Cu+Laser, CaO_2@PDA-Cu@MnCO+Laser). Afterward, the cells were stained with DCFH-DA (10 μM) at 37 ℃. The intracellular fluorescence was visualized on a fluorescence microscope.

In vitro toxicity assay

4T1 cells were cultured in 96-well plates. When the growth rate of 4T1 reached about 80%, the culture medium was sucked out, and fresh DMEM containing PBS, CaO_2@PDA, CaO_2@PDA-Cu, CaO_2@PDA-Cu@MnCO, CaO_2@PDA+L, CaO_2@PDA-Cu+L, CaO_2@PDA-Cu@MnCO+L material groups with different concentrations were added. After incubation for 24 h, the culture medium was replaced by 100 μL CCK-8 (0.1 mg/mL). Following a 4-hour incubation. The absorbance of each hole of the 96-well plate at 450 nm was detected using an enzyme marker.

Live-dead cell staining

4T1 cells were seeded into 12-well plates for 24 h and incubated with samples (CaO_2, CaO_2@PDA, CaO_2@PDA-Cu, CaO_2@PDA-Cu@MnCO) in the absence and presence of 808 nm laser (1.0 W cm^{-2}) irradiation. After that, the 4T1 cells were further incubated for 6 h and then stained with Calcein-AM/PI for 30 min. Lastly, the treated cells were washed with PBS for several times and imaged by a fluorescence microscope.

Detection of Mitochondrial Membrane Potential (MMP)

After diverse treatments (similar with those in live-dead cell staining), 4T1 cells were co-incubated with JC-1 probe (5.0 μg mL^{-1}) for 20 min. Then, the cells were washed three times with JC-1 buffer. The fluorescence of JC-1 monomers (490–540 nm) and aggregates (560–630 nm) in cytoplasm was recorded on a CLSM.

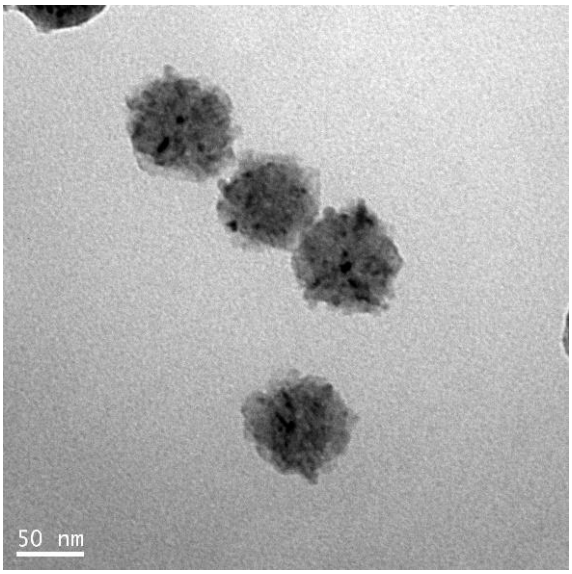

Fig. S1 TEM image of the prepared CaO_2 NPs.

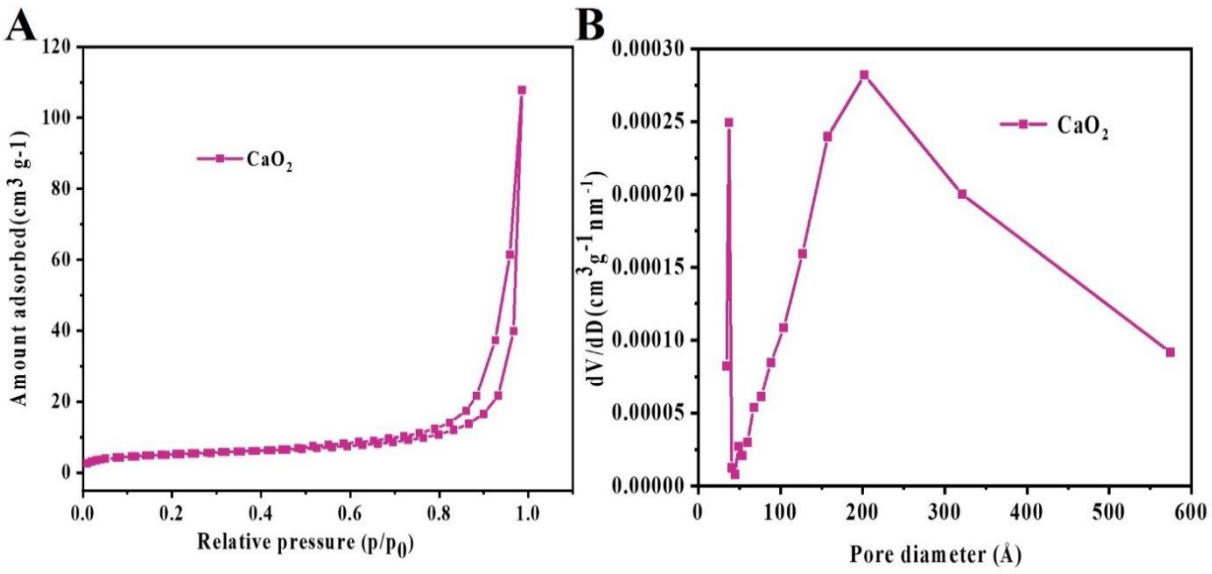

Fig. S2 (A) Pore sizes and (B) N_2 adsorption and desorption isotherm of the prepared CaO_2 NPs

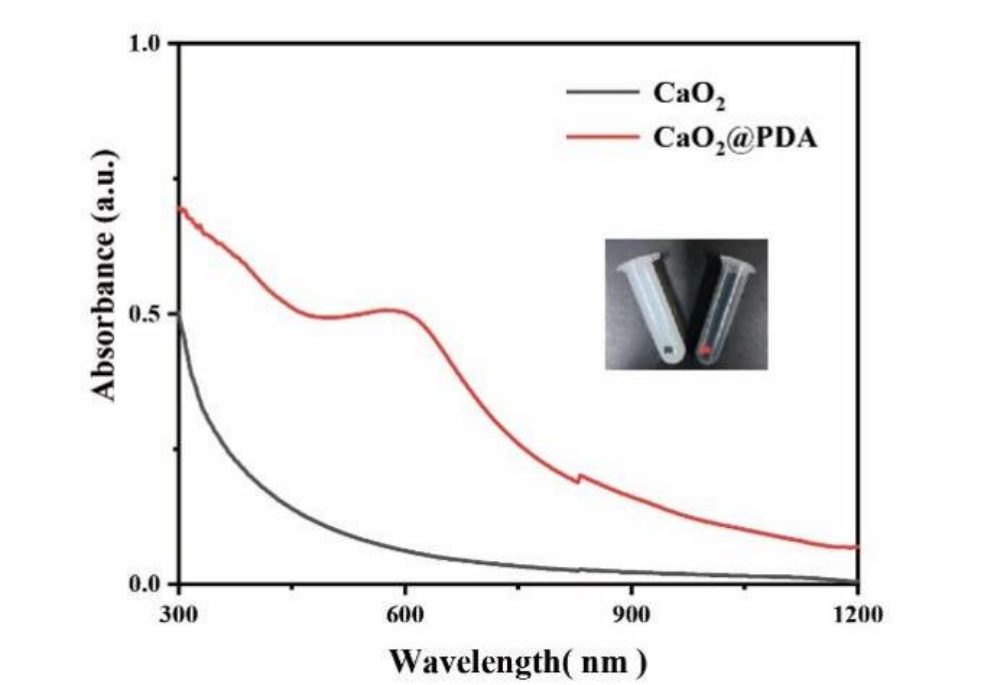

Fig. S3 UV-vis absorption spectra of the solution of CaO_2 and CaO_2@PDA.

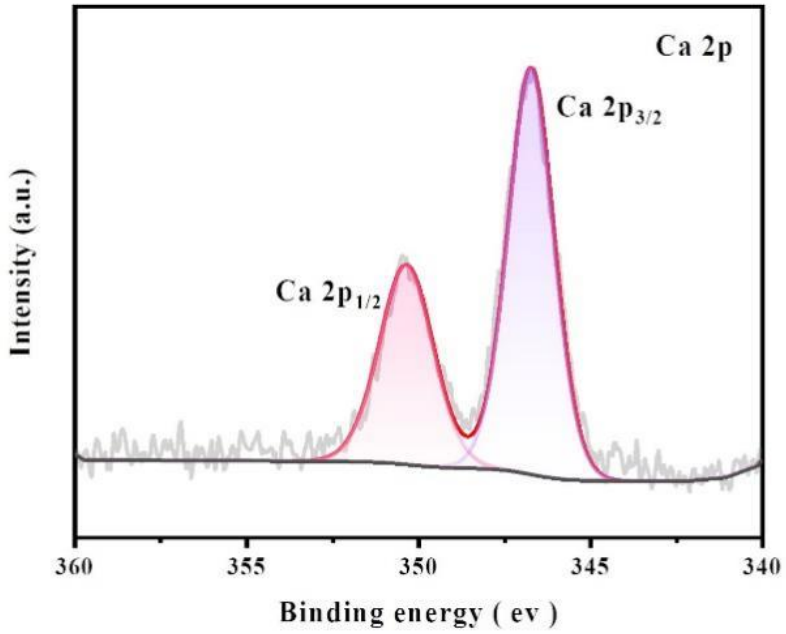

Fig. S4. High resolution Ca 2p XPS spectra of CaO_2@PDA-Cu@MnCO.

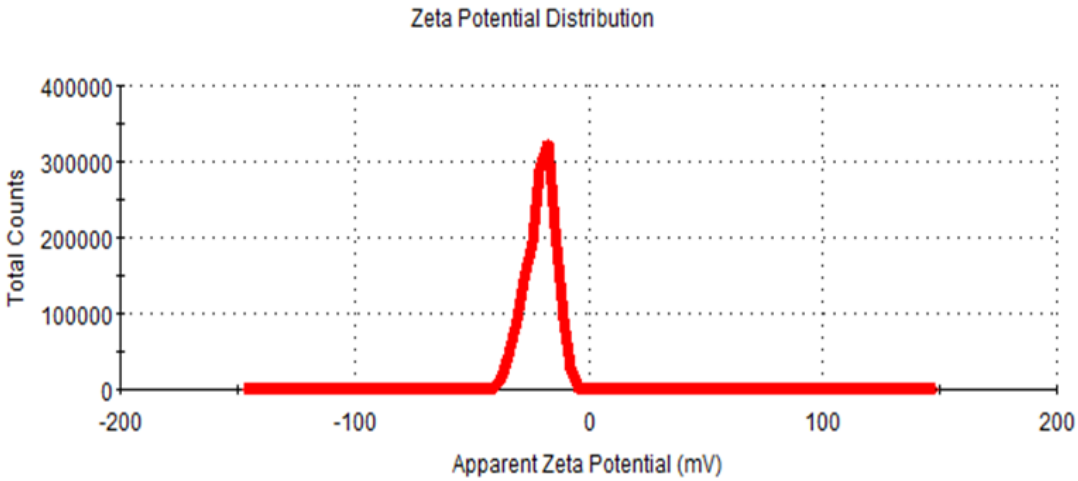

Fig. S5 Surface Zeta potential distribution of CaO_2@PDA-Cu@MnCO NPs.

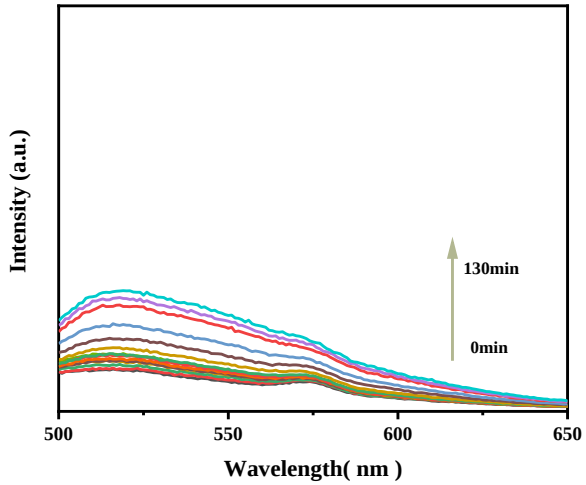

Fig. S6 Variation curves of CO release from CaO_2@PDA-Cu@MnCO at different times using the FL-CO-1 probe in the presence of 5 μM H_2O_2.

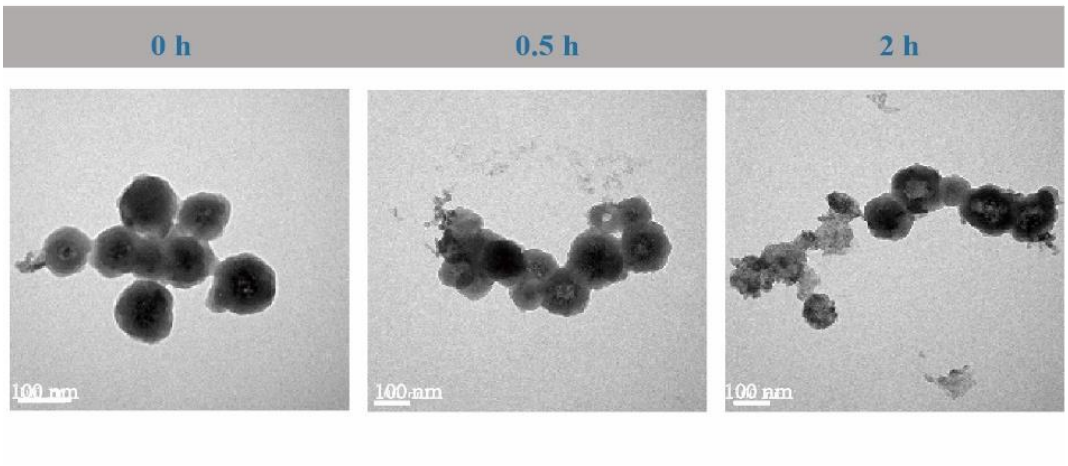

Fig. S7 TEM images of CaO_2@PDA-Cu@MnCO in PBS solutions (pH 6.5).

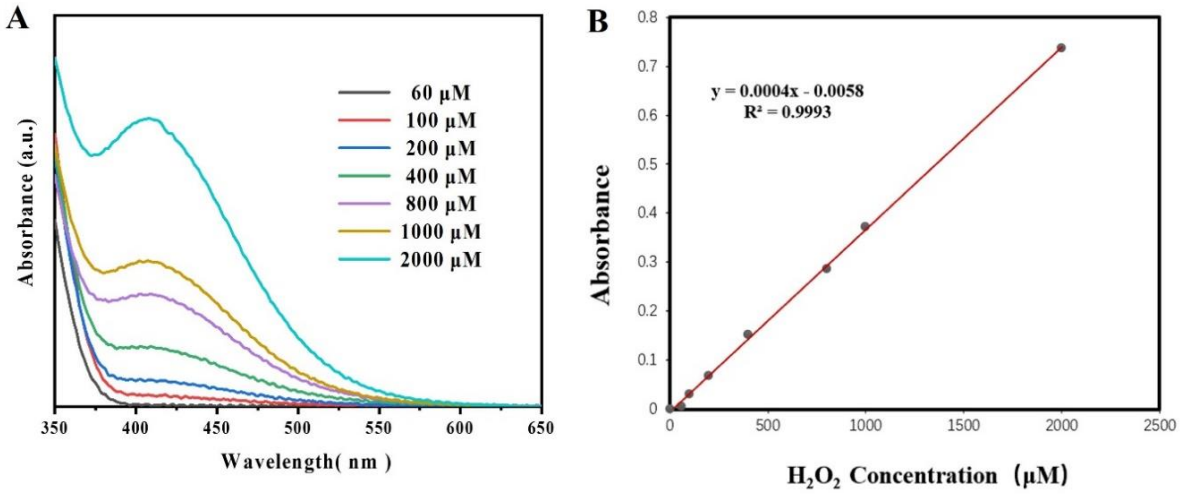

Fig. S8 (A) UV–vis absorption spectra of Ti $(SO_4)_2$ solution mixed with various concentrations of H_2O_2; and (B) Plot of absorbance versus concentrations of H_2O_2 based on different absorbance at 410 nm.

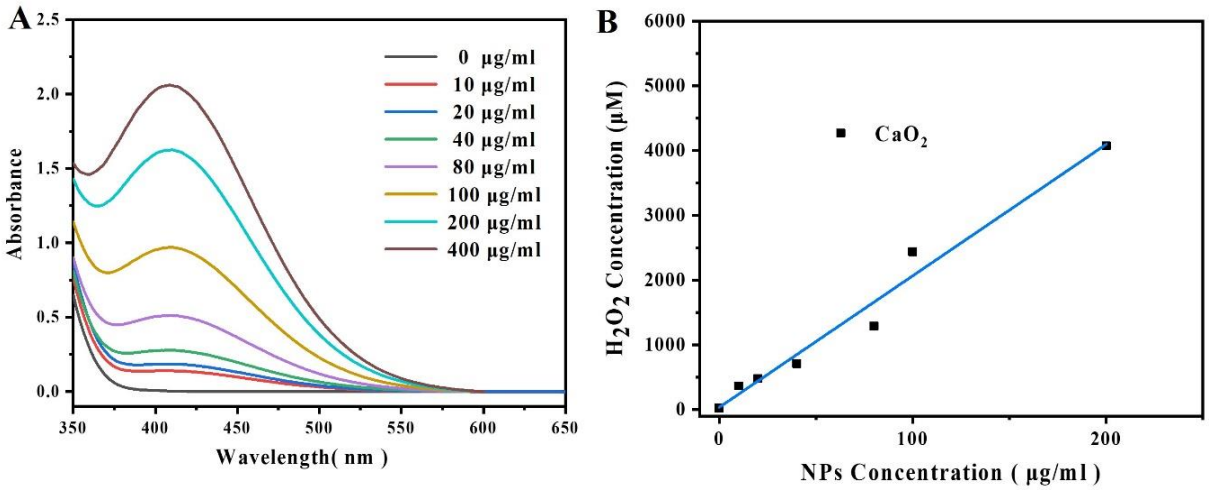

Fig. S9 (A) UV–vis absorption spectra of Ti $(SO_4)_2$ solution mixed with various concentrations of CaO_2 NPs; (B) Plot of CaO_2 NPs concentration versus H_2O_2 concentration based on different absorbance at 410 nm.

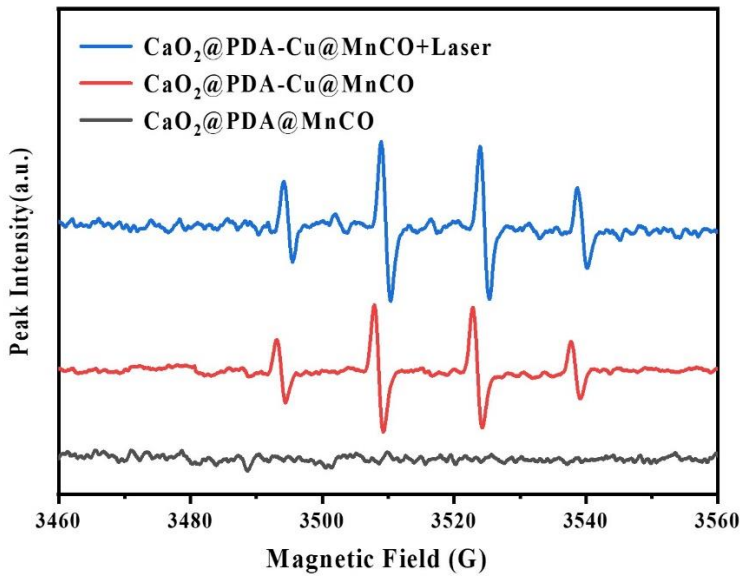

Fig. S10 ESR spectra of DMPO in the presence of CaO_2@PDA@MnCO and CaO_2@PDA-Cu@MnCO, respectively, treated under different conditions. (Laser: 808 nm, 1.0 W/cm^2)

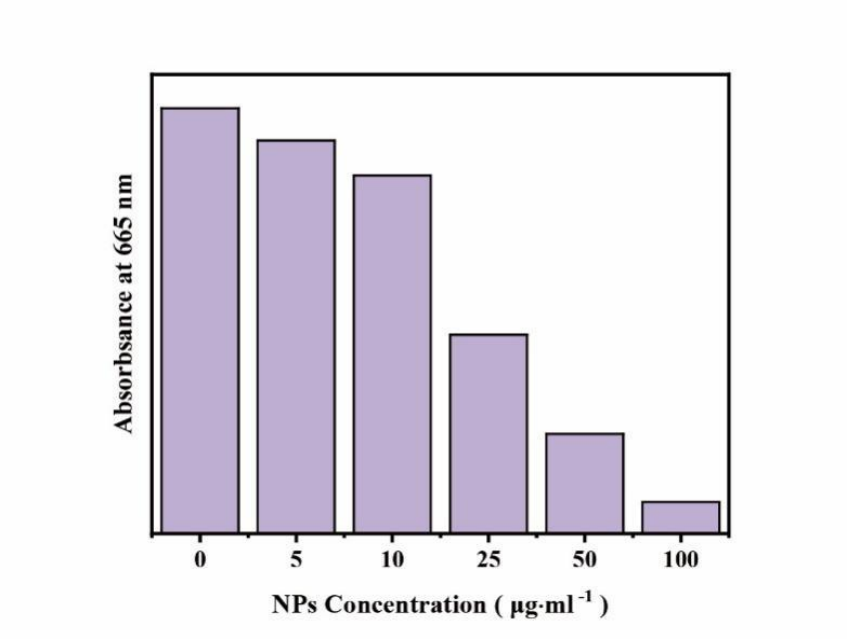

Fig. S11 Absorbance at 665 nm of MB solution treated with different concentrations of CaO_2@PDA-Cu.

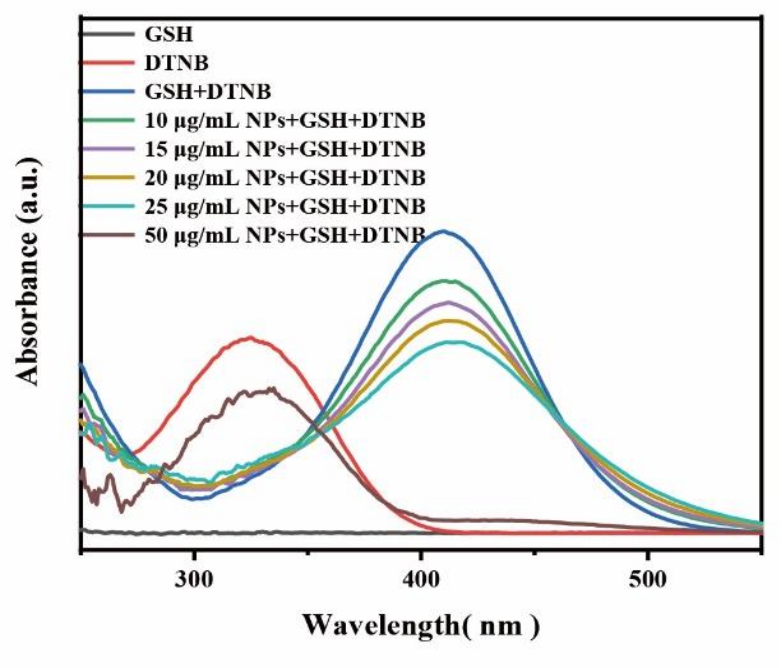

Fig. S12 GSH depletion by different concentrations of CaO_2@PDA-Cu.

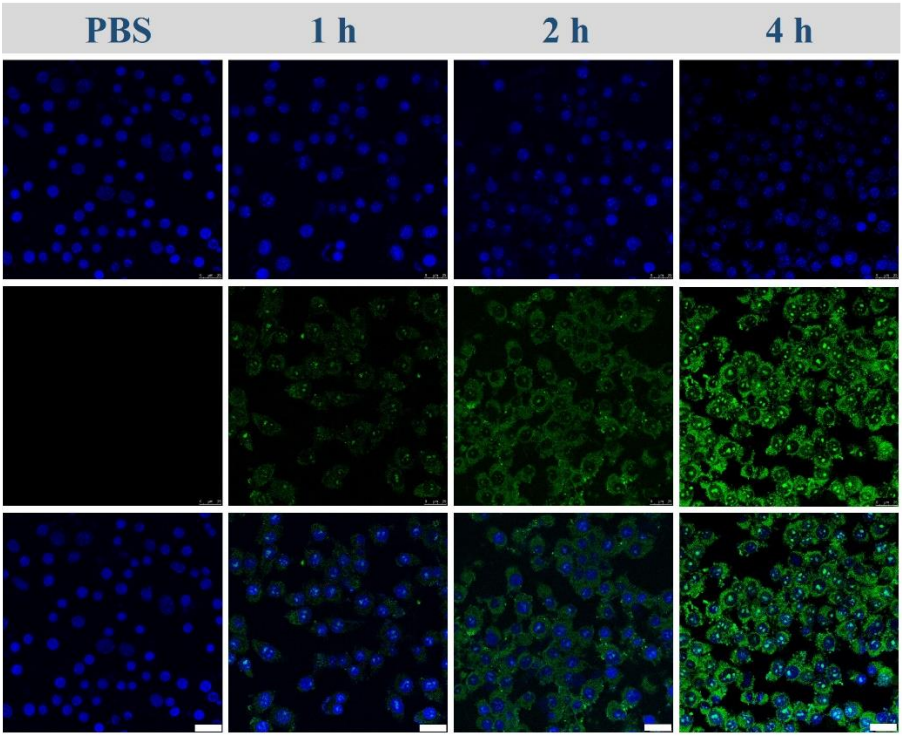

Fig. S13 The fluorescence intensity of FITC labled CaO_2@PDA-Cu@MnCO in 4T1 cells with different time was detected by CLSM. Cells were stained with DAPI (blue). Scar Bar:25 μm.

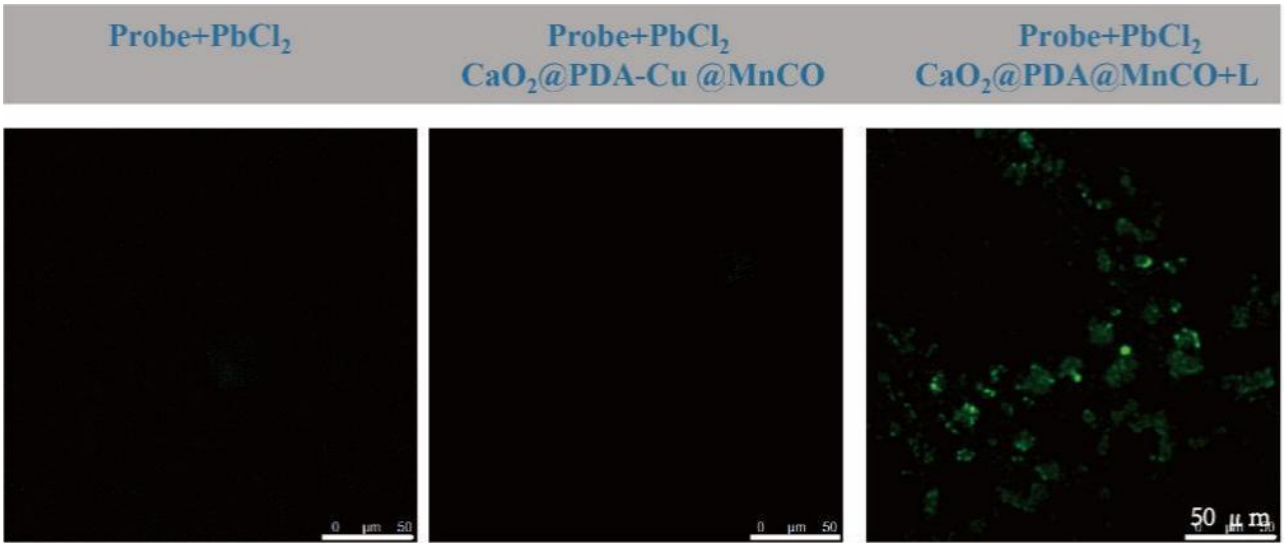

Fig. S14 Confocal microscopic images of 4T1 cells co-incubated with the probe system (FL-CO-1 + $PdCl_2$, scale bar 50 μm) and CaO_2@PDA-Cu@MnCO in the absence and presence of 808 nm light irradiation (1.0 W/cm^2).

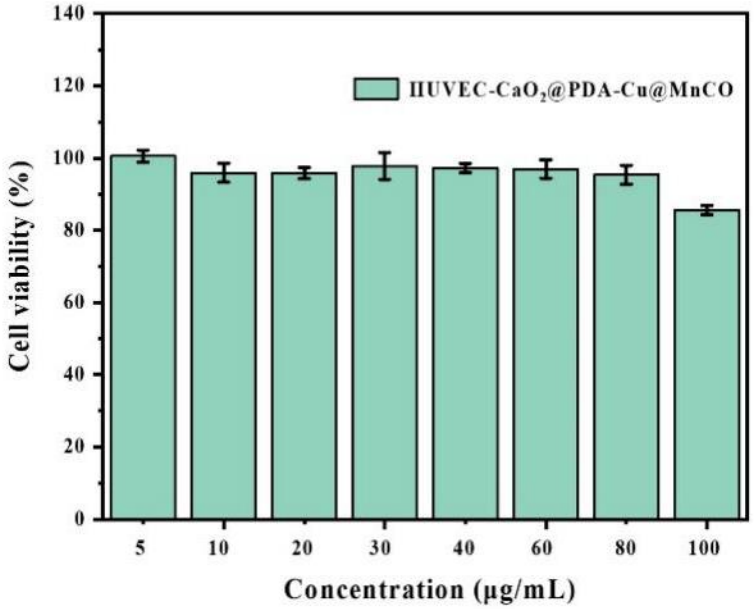

Fig. S15 Cell viability of HUVEC cells incubated with different concentrations of CaO_2@PDA-Cu@MnCO for 24 h;

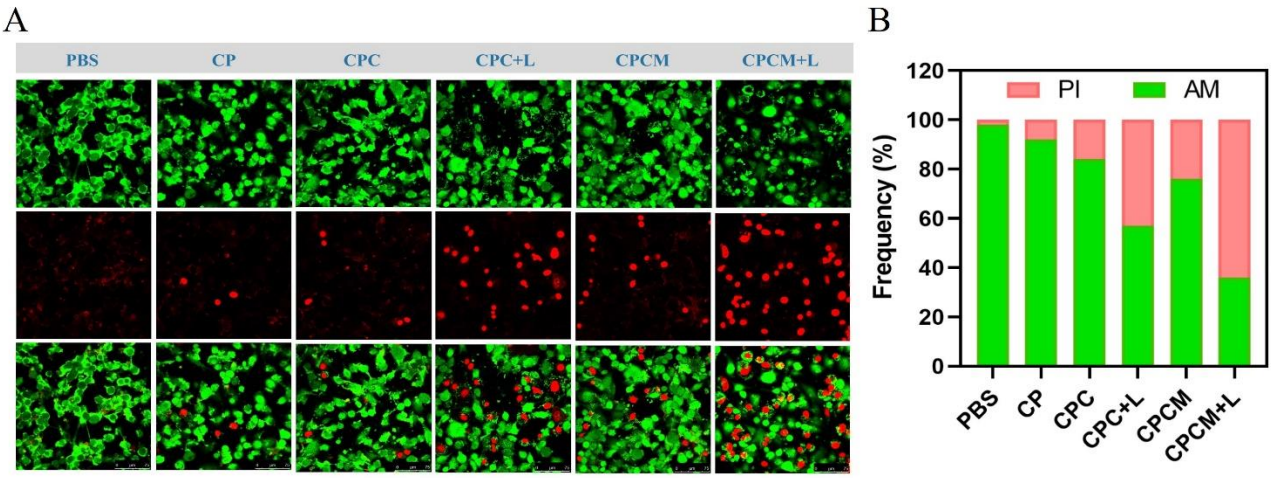

Fig. S16 (A) Fluorescent images of Calcein-AM/PI stained 4T1 cells with various treatments (scale bar = 75 μm); (B) Semi quantitative statistics of intracellar AM/PI corresponding to (A).

References

S1 Q. Tang, J. Liu, C. B. Wang, L. An, H. L. Zhang, Y. Wang, B. Ren, S. P. Yang and J.-G. Liu, *Nanoscale*, 2022, ***14***, 9097-9103.

S2 H. L. Zhang, Y. Wang, Q. Tang, C. B. Wang, M. J. Chen, S. P. Yang and J.-G. Liu, *Colloids Surf. B. Biointerfaces*, 2023, ***230***, 113513.

S3 T. Pan, W. Fu, H. Xin, S. Geng, Z. Li, H. Cui, Y. Zhang, P. K. Chu, W. Zhou and X. F. Yu, *Adv. Funct. Mater.*, 2020, ***30***, 2003069.